Rare Met. (2021) 40(9):2593–2601
https://doi.org/10.1007/s12598-020-01695-9

RARE METALS

ORIGINAL ARTICLE

GNPs/Al nanocomposites with high strength and ductility and electrical conductivity fabricated by accumulative roll-compositing

Zi-Hao Chen, Han-Yu Hui, Cheng-Lin Li*, Feng Chen, Xin-Ming Mei, Ye Ma, Ju-Ying Li, Seong-Woo Choi, Qing-Song Mei*

Received: 22 October 2020 / Revised: 14 November 2020 / Accepted: 20 November 2020 / Published online: 25 February 2021

Abstract Aluminum matrix composites (AMCs) reinforced with graphene nanoplatelets (GNPs) were fabricated by using an accumulative roll-compositing (ARC) process. Microstructure, mechanical and electrical properties of the nanostructured AMCs were characterized. The results showed that small addition (0.2 vol% and 0.5 vol%) of GNPs can lead to a simultaneous increase in the tensile strength and ductility of the GNPs/Al nanocomposites, as compared with the same processed pure Al. With increasing GNPs content, the tensile strength of the GNPs/Al nanocomposites can be enhanced to 387 MPa with retained elongation of 15%. Meanwhile, the GNPs/Al nanocomposites exhibited a good electrical conductivity of 77.8%–86.1% that of annealed pure Al. The excellent properties (high strength, high ductility and high conductivity) of the GNPs/Al are associated with the particular ARC process, which facilitates the uniform dispersion of GNPs in the matrix and formation of ultrafine-grained Al matrix. The strengthening and toughening of the GNPs/Al nanocomposites were discussed considering different mechanisms and the unique effect of GNPs.

Z.-H. Chen, H.-Y. Hui, C.-L. Li*, F. Chen, X.-M. Mei, Y. Ma, Q.-S. Mei*
School of Power and Mechanical Engineering, Wuhan University, Wuhan 430072, China
e-mail: lichenglin211@whu.edu.cn

Q.-S. Mei
e-mail: qsmei@whu.edu.cn

J.-Y. Li
School of Mechanical Engineering, Wuhan Polytechnic University, Wuhan 430023, China

S.-W. Choi
Advanced Metals Division, Korea Institute of Materials Science, Changwon 51508, Republic of Korea

Keywords Aluminum matrix composites; Graphene nanoplatelets; Accumulative roll compositing; Electrical conductivity; Mechanical properties

1 Introduction

Conventional aluminum matrix composites (AMCs) reinforced with ceramic particles exhibit high specific strength and elastic modulus over their monolithic alloys [1, 2]. Those AMCs have been widely used as structural materials in aerospace and automotive industries [3]. There are some issues connected with these ceramic particles such as large size, large volume fraction addition, formation of weak interface with metals, brittle nature and undesired agglomeration during their processing [4, 5]. These issues are barriers to the implementations of AMCs in the industry [6]. Compared with ceramic reinforcements, nanocarbons such as carbon nanotubes (CNTs) and graphene are attractive reinforcing materials to fabricate high-performance nanocomposites because of their superior mechanical and physical properties [7]. Nanocomposites reinforced with CNTs or graphene have emerged as an important class of new materials for structural engineering and functional device applications because of their extraordinary high elastic modulus and mechanical strength as well as excellent electrical and thermal conductivities [7]. In combination with their high aspect ratio characteristics, CNTs and graphene are the most effective reinforcements for metal matrices such as Al [8–10], Cu [11] and Mg [12, 13].

It has been reported that AMCs reinforced with CNTs offer high strength and high conductivity [9, 14–16]. In recent years, graphene has attracted much attention as a

better substitute for CNTs in AMCs. Graphene nanoplatelets (GNPs) reinforced AMCs were prepared by ball milling, hot isostatic pressing and extrusion; however, the graphene/Al composites exhibited lower strength than pure Al and CNTs/Al composites because of the formation of Al_4C_3 [17]. Graphene nanosheets reinforced AMCs were fabricated through powder metallurgy, compacting and extrusion [18]. The tensile strength of the AMC reinforced with 0.3 wt% graphene nanosheets was 249 MPa, of 62% enhancement over pure Al matrix, indicating that graphene nanosheets can actually act as effective reinforcements in Al [18]. Li et al. [19] fabricated AMCs reinforced with graphene nanoflakes (GNFs: 0 wt%–2 wt%) by cryo-milling and hot extrusion. They reported that the tensile strength of the composites with 0.5 wt% GNFs significantly improved from 150 (unreinforced Al) to 175 MPa, whereas the elongation increased from 17.3% to 19.9% simultaneously. They explained that the improved ductility was because that the wrinkled GNFs were straightened and flattened during plastic deformation. On the contrary, the mechanical properties significantly deteriorated due to the agglomeration of graphene when GNFs content exceeded 1 wt%. Gao et al. [20] reported that the graphene-reinforced AMCs fabricated with graphene oxide through powder metallurgy exhibited a tensile elongation as high as 30%–40%, but the tensile strength was not encouraging ($\sim$ 100 MPa). Among the graphene-based AMCs as have been reported so far, the highest tensile strength of 440 MPa was obtained in AMCs reinforced with 0.7 vol% few-layer graphene; however, its elongation was as low as 3% [21]. In contrast with the mechanical properties, few information of the electrical properties of the graphene-reinforced AMCs is available in the literature. Recently, Li et al. [22] prepared GNPs reinforced AMCs by continuous casting and subsequent rolling. The electrical conductivity of the composites (0.2 wt% GNPs) was up to 37.2 $MS{\cdot}m^{-1}$, which was slightly higher than that of annealed pure Al; however, the tensile strength and elongation were 156 MPa and 4%, respectively. In view of their microstructures, obtaining a uniform dispersion of GNPs in Al is still a great challenge due to the agglomeration of graphene, especially for a large amount of addition.

It is usually difficult to obtain a uniform dispersion of nanocarbon reinforcements (CNTs or GNPs) into Al matrix because they can easily agglomerate into clusters. Another issue arises from the poor wetting of GNPs or CNTs due to a large difference in the surface tension between them and Al. In addition, formation of aluminum carbide (Al_4C_3) is commonly observed, which is an undesired phase in terms of mechanical performance [9, 14, 23, 24]. Therefore, it is a great challenge to fabricate high-performance GNPs/Al composites by using conventional melting-based methods such as stirring casting, squeeze casting or using powder metallurgy.

The homogeneous distribution of graphene reinforcements in the matrix is a prerequisite to obtaining desired enhancement of mechanical and electrical properties. Controlling the undesired phase (Al_4C_3) is important because the Al_4C_3 formation along the graphene/Al interfaces adversely affects the composite strength. Moreover, it is advantageous to retain nanosized Al matrix grains, which can lead to significant improvement in hardness, strength and wear resistance of composites. In consideration of such problems, advanced process and microstructural control are still challenging for fabrication of graphene/Al nanocomposites. Our previous studies [25, 26] have demonstrated that using proper accumulative roll-bonding process enabled to fabricate Al matrix nanocomposites with a homogenous distribution of ceramic nanoparticles in the Al matrix. In this study, a similar accumulative roll-compositing (ARC) process performed at room temperature and at high temperature was applied to fabricate GNPs/Al nanocomposites. The microstructures, mechanical properties and electrical conductivity of the GNPs/Al nanocomposites were investigated. The strengthening mechanisms and the characteristic of high strength and high conductivity were discussed.

2 Experimental

2.1 Fabrication of GNPs/Al nanocomposites

The raw materials used in this study were pure Al sheets (purity of 99.99 wt%) and GNPs (purity > 99.5 wt%). The Al sheets were purchased from China New Metal (Beijing, China) and the GNPs from Times Nano (Chengdu, China). The as-received Al sheets were first annealed at 400 °C for 2 h and the microstructure consisted of equiaxed grains with an average size of 87 μm. The GNPs exhibited a size of 5–10 μm and a thickness of 4–20 nm (Fig. 1).

The ARC process was used to fabricate GNPs/Al composites. The Al sheets (125 mm^L × 25 mm^W × 0.25 mm^T) were brushed with a stainless steel brush to remove the oxidation of the surfaces and then were ultra-sonicated in anhydrous ethanol to remove the impurities. The GNPs were first ultra-sonicated in anhydrous ethanol for 10 min. The dispersed GNPs ethanol solution was uniformly spread on the surfaces of the Al sheets. Eight pieces of the Al sheets with the dried GNPs were stacked and clamped by using a stainless-steel envelope to avoid sliding during rolling. The GNPs/Al samples having different volume fraction (V_f) of GNPs from 0% to 2% were prepared. They are referred to as Samples S1–S5 hereinafter as shown in Table 1. The ARC process was carried out by using a

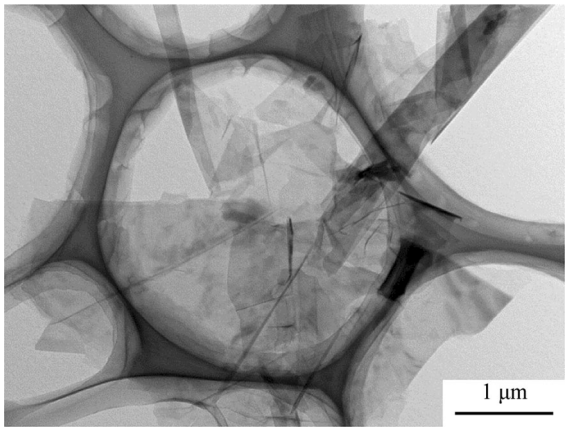

Fig. 1 TEM image of initial GNPs

Table 1 Processing parameters of samples

Sample	GNPs addition/vol%	ARC cycles (*n*)	ARC at high temperature		
			Temperature/°C	Time/min	Cycles (*n*)
S1	0	150	600	30	3
S2	0.2	150	600	30	3
S3	0.5	150	600	30	3
S4	0.5	150	500	10	3
S5	2.0	5	600	10	1
		22	600	10	1
		135	600	30	3

laboratory roller with two rolls (Φ205 mm) and at a speed of 10 r·min^{-1}. The initial GNPs/Al sandwiches were rolled at room temperature to obtain a total thickness reduction of 50% for each cycle through multiple passes. The roll-bonded samples after each cycle were folded in half and rolled again. A total number of rolling cycles of 150 were applied at room temperature. After that, the samples were heat-treated at 500 °C for 10 min or 600 °C for 30 min before each cycle of rolling; a total cycle of 3 was applied with a thickness reduction of 40% for each cycle. Sample S5 was fabricated by using a different procedure owing to the high V_f of GNPs. The detailed processing parameters are listed in Table 1.

2.2 Characterizations

Microstructures of the raw GNPs were characterized by using transmission electron microscopy (TEM, JEM-2100HT). Microstructures of the Al sheets and the GNPs/Al samples were observed by using optical microscopy (OM) and scanning electron microscopy (SEM, TESCAN MIRA 3 LMH). Electron channeling contrast imaging (ECCI) technique was used to take images of the nano-grain structure of the GNPs/Al samples. The rolling direction (RD)–normal direction (ND) planes of the composite samples were mechanically ground and polished for the OM and SEM observations. The samples for OM observation were etched in a 5% hydrofluoric acid aqueous solution for 30 s. X-ray diffraction (XRD) was used to analyze the crystal structure of the composite samples. XRD measurements were carried out by using a Cu-based X-ray diffraction instrument (XRD, XPert Pro X) with scanning in the range of 30°-80° at 40 kV and 40 mA.

Microhardness measurements were carried out on the RD-ND planes of the samples by using an HVS–1000A microhardness tester under a load of 0.98 N for a duration time of 10 s; 12 points of each sample were measured, and their average values were reported. Tensile tests were performed at room temperature by using an MTS E45 universal testing machine, at a strain rate of 1.4×10^{-3} s^{-1}. Dog-bone-shaped specimens were cut along the RD and had a gauge length of 6 mm, a gauge width of 2 mm and a gauge thickness of 1 mm. Three specimens of each sample were tested, and their average values were reported. Electrical conductivities of the composite samples were measured on the ND plane by using a FOR7051A eddy current conductometer. Each sample was measured 10 times, and the average values were reported.

3 Results

3.1 Microstructures

XRD patterns of the ARCed samples are shown in Fig. 2. As shown in Fig. 2, only Al peaks were detected and no formation of carbides (Al_4C_3) was observed in all the samples. It has been reported that the Al_4C_3 is a brittle phase and has a negative influence on the mechanical properties of the composites [17]. Our results show that the present ARC process operated at a temperature as high as 600 °C did not introduce the undesirable Al_4C_3 phase, which is beneficial for the mechanical properties of the GNPs/Al composites.

Figure 3 shows the OM images of the ARCed GNPs/Al samples. It is observed that all the samples were well bonded without any obvious holes and microcracks. In the GNPs/Al samples, the GNPs were uniformly distributed in the Al matrix though the content of GNPs reached 2%. The electron channeling contrast (ECC) images in Fig. 4 show the grain structure of the Al matrix in all samples. The ARC process resulted in the formation of equiaxed ultra-fine grains (UFG) of the matrix. As shown in Fig. 4f, enhanced grain refinement was observed in the GNPs/Al samples owing to the addition of the GNPs. For instance,

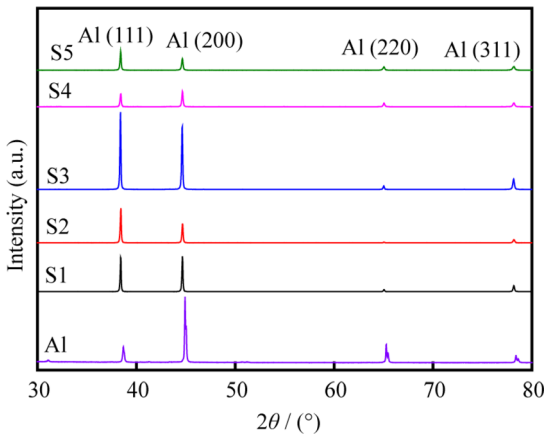

Fig. 2 XRD patterns of GNPs/Al samples as indicated

Sample S1 (pure Al) exhibited a grain size of 615 nm, whereas Samples S2–S4 exhibited grain sizes ranging from 461 to 333 nm. In particular, Sample S5 exhibited the finest grain size of 238 nm due to the lower temperature and the shorter time during the heat treatment.

Figure 5 shows the morphologies of the GNPs in the GNPs/Al samples. To better identify the GNPs, the samples were etched for SEM observation. The corresponding energy-dispersive spectroscopy (EDS) maps in Fig. 5 can verify the existence of the carbon-rich regions, which are related to the GNPs. In particular, some GNPs were thinned and some GNPs still retained the original fold shape. It is also seen that while most of the GNPs tend to distribute along the RD, GNPs aligned to the normal direction can be observed, as shown in Fig. 5c.

3.2 Mechanical properties

Figure 6 shows the microhardness of the annealed pure Al and the ARCed samples. Sample S1 (ARCed pure Al) exhibited a hardness of HV 52.7, ~ 1.8 times that of the pure Al sample. With increasing GNPs content, the microhardness of the composite samples increased from HV 52.7 to HV 103.1, indicating the synergistic strengthening effect of grain refinement and GNPs reinforcement. It is seen that Sample S4 has a higher hardness than Sample S3 though they have the same content of GNPs (0.5 vol%). This can be attributed to the difference in the heat treatment during the ARC process; namely, the lower temperature (500 °C) applied for Sample S4 resulted in refined grain size, as shown in Fig. 4c, d.

Figure 7a shows the typical engineering stress–strain curves of the annealed pure Al and ARCed samples. The annealed pure Al sample exhibited a low ultimate tensile strength (UTS) of 81 MPa and high ductility (elongation (El) of 50%). Compared with the annealed Al sample, the ARCed samples exhibited improved strength and decreased ductility. Sample S1 (ARCed pure Al) exhibited improved

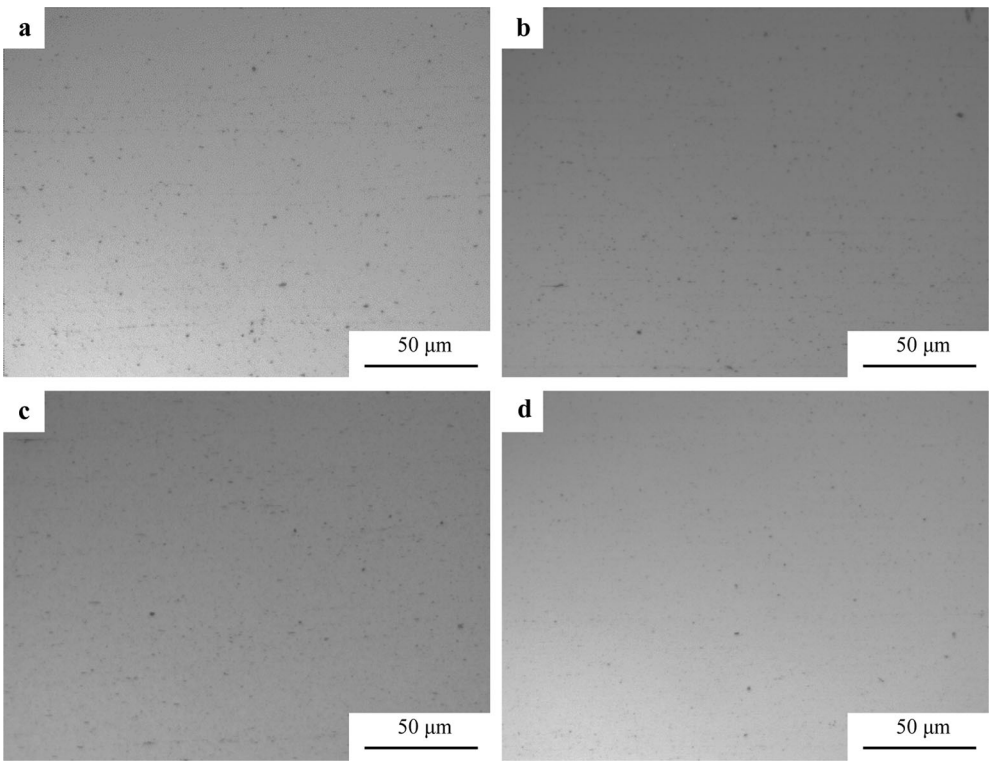

Fig. 3 OM images of ARCed GNPs/Al Samples **a** S2, **b** S3, **c** S4 and **d** S5

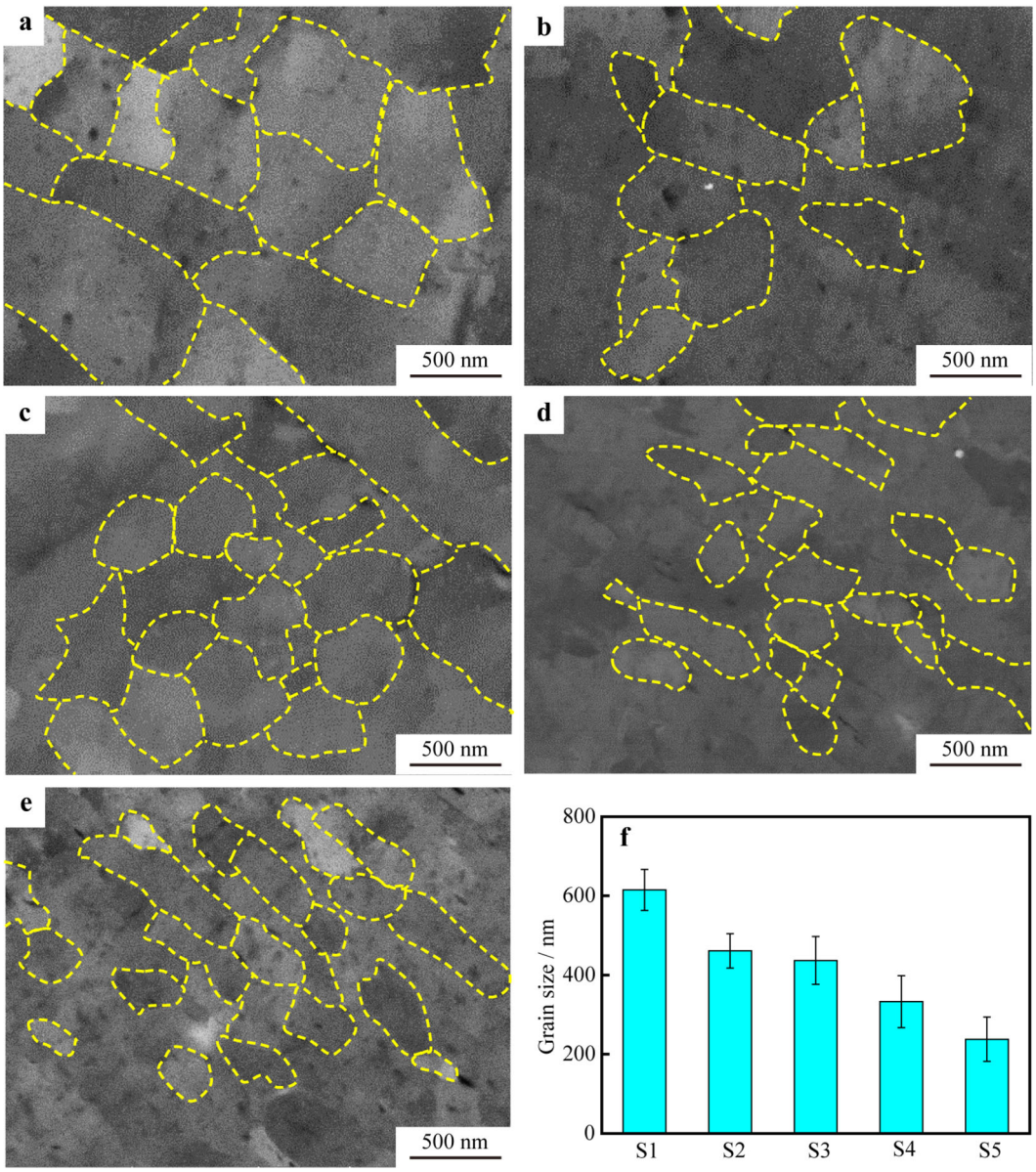

Fig. 4 ECC images of ARCed Samples **a** S1, **b** S2, **c** S3, **d** S4, **e** S5 and **f** grain size of ARCed samples

strength (UTS: 181 MPa) and decreased ductility (El: 13.5%). With increasing GNPs addition, the strength of the composite samples increased. This is consistent with the microhardness measurements as shown in Fig. 6. Interestingly, it is seen that the small amount of GNPs addition can result in both improved strength and ductility. As shown in Fig. 7a, Samples S2 (0.2 vol% GNPs) and S3 (0.5 vol% GNPs) exhibited both enhanced strength and ductility as compared with Sample S1. This indicates the unique effect of GNPs on the deformation of the composites. Figure 7b illustrates the combination of strength and ductility of the present GNPs/Al composites, as compared with other graphene reinforced AMCs [18–22, 27–29]. As shown in Fig. 7b, the present GNPs/Al composites exhibited an excellent combination of strength and ductility, with strengths ranging from 250 to 380 MPa and Els of 14%–20%. The strength–ductility combination of the present GNPs/Al samples is better than those reported in Refs. [18–22, 27–29].

3.3 Electrical conductivity

Figure 8a shows the electrical conductivity of the pure Al sample and ARCed samples. Compared with annealed pure Al and ARCed Al samples, a slight decrease in the electrical conductivity is observed in the GNPs/Al samples due to the interface electrical resistance between GNPs and Al. The electrical conductivities of the Samples S2–S5 are 31,

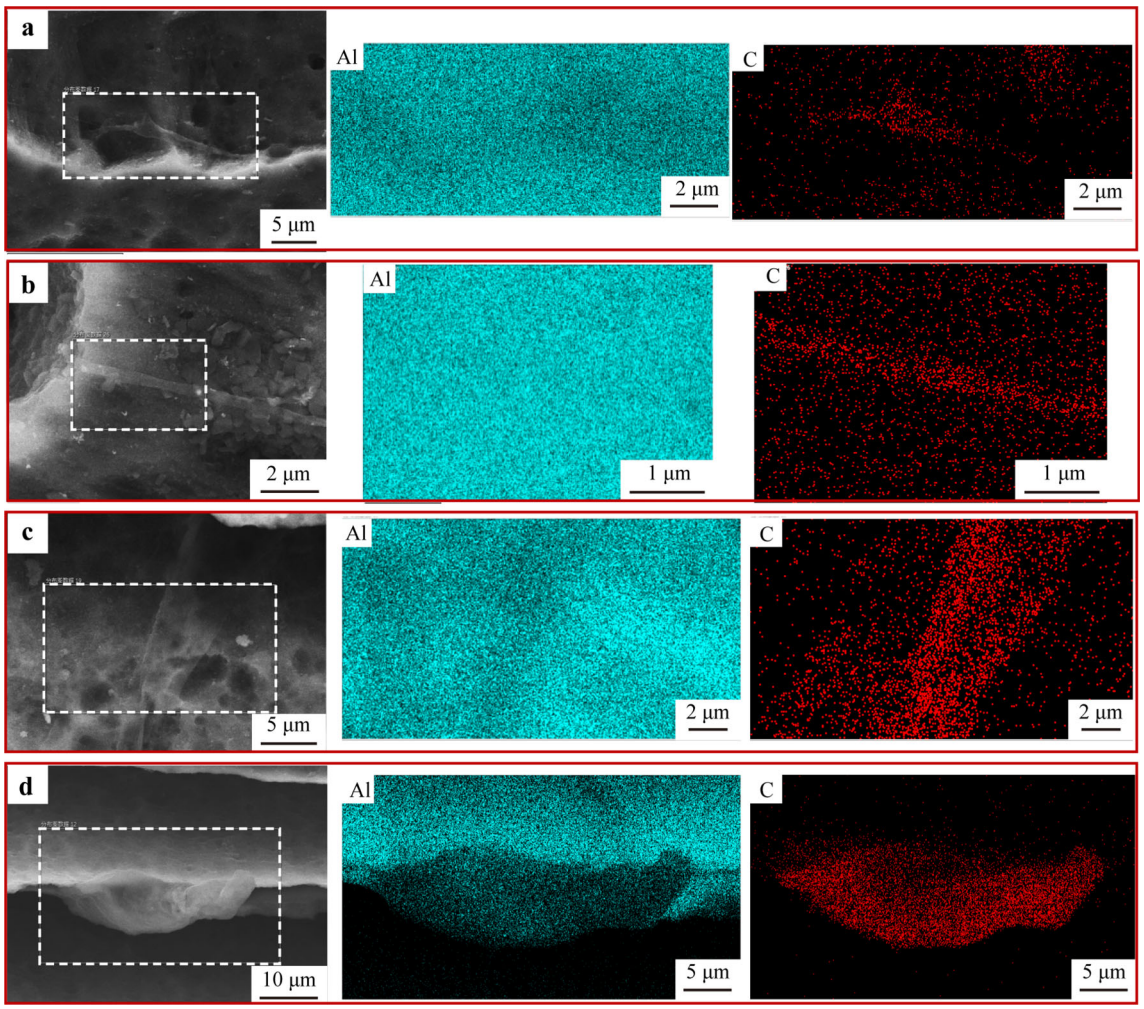

Fig. 5 Morphologies of GNPs and corresponding EDS mappings in composite Samples **a** S2, **b** S3, **c** S4 and **d** S5

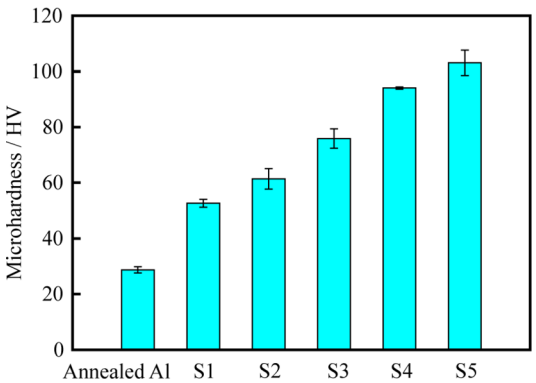

Fig. 6 Microhardness of pure Al sample and ARCed samples

30, 28 and 30 MS·m^{-1}, respectively. Figure 8b represents the tensile strength and electrical conductivity of the present samples, as compared with other AMCs (GNPs/Al [22] and CNTs/Al [16]) and Al alloys [30, 31]. It is observed that conventional Al alloys exhibited moderate or high strength (200–600 MPa) but much reduced conductivity (15–25 MS·m^{-1}) [30–33]. The CNTs/Al composites exhibited high conductivity (37 MS·m^{-1}) but low strength [16]. The GNPs/Al composite (0.2 wt%) had an electrical conductivity of 37.2 MS·m^{-1} but a low tensile strength of 156 MPa [22]. The present GNPs/Al composites exhibited a well-balanced strength (250–387 MPa) and electrical conductivity (28–31 MS·m^{-1}), as shown in Fig. 8b.

4 Discussion

The experimental results suggest that the present ARC process enabled the fabrication of GNPs/Al nanocomposites with an excellent balance of mechanical properties (strength and ductility) and electrical conductivity. Based on our findings, the combined effect of the ARC process and GNPs addition is considered.

First, enhanced strength can be achieved by a finer grain structure according to the Hall–Petch relation [25]. The

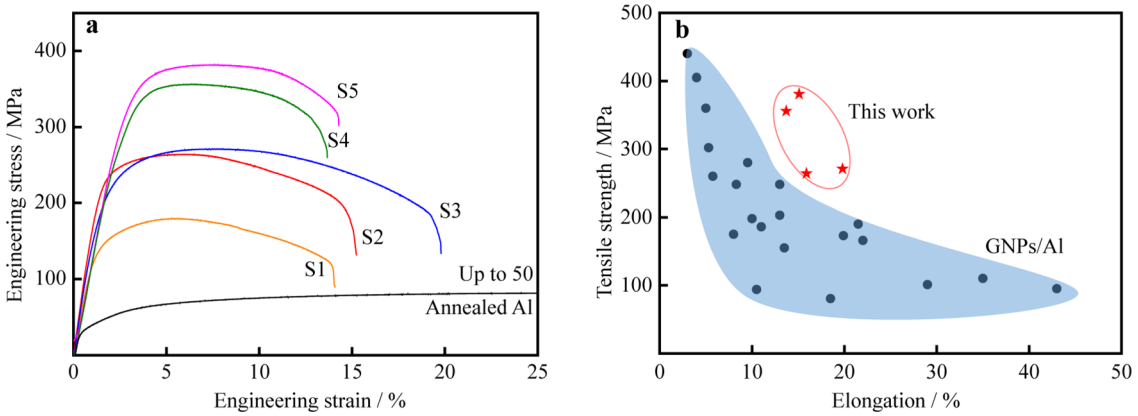

Fig. 7 **a** Typical engineering stress–strain curves of present GNPs/Al samples; **b** UTS and El combination of present GNPs/Al samples as compared with literature results [18–22, 27–29]

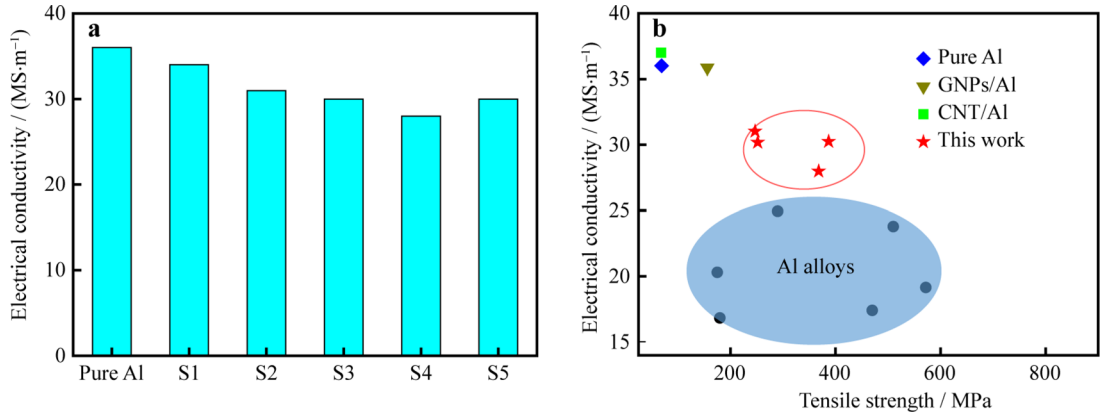

Fig. 8 **a** Electrical conductivity of pure Al and Samples S1-S5; **b** tensile strength-electrical conductivity of present GNPs/Al samples in comparison with GNPs/Al [22] and CNTs/Al [16] composites and Al and Al alloys [30, 31]

present ARC process resulted in significant grain refinement of pure Al, resulting in a UFG structure with grain size of ~ 615 nm in Sample S1. This gave rise to improved strength of 170 MPa in Sample S1, about twice that of the annealed coarse-grained pure Al sample (80 MPa). Apart from the ARC-induced grain refinement, the presence of GNPs also had a significant influence on the grain refinement, as GNPs can enhance the strain-induced grain refinement and hinder the grain growth of the Al matrix during ARC process. The grain size decreased to 238 nm with increasing GNPs addition in the GNPs/Al samples (Fig. 4). The further grain refinement from GNPs contributed an extra strengthening of approximately 45-77 MPa based on the Hall–Petch relation.

Second, the ARC process resulted in a homogeneous distribution of GNPs with minimal agglomeration in the Al matrix. The high strengthening efficiency of GNPs originates mainly from the high surface area and high aspect ratio of GNPs. Therefore, the uniform distribution of GNPs in the present composites is the key for sufficient utilizing the unique strengthening of GNPs, which can give rise to a significant contribution due to interfacial strengthening and load transfer effect [21, 34].

Third, the high ductility in the samples can be attributed to GNPs bridging, pulling out and flattening on crack propagation. As shown in Fig. 9, GNPs bridging between the Al layers can delay crack propagation, which could have a contribution to the ductility improvement [35]. In the case of tensile deformation, GNPs were pulled out from the matrix, the energy is largely dissipated by interface debonding and subsequent friction [36, 37]. The GNPs with a multiply and highly wrinkled structure are straightened and flattened during plastic deformation. The flattening of GNPs can also delay the fracture of composites, which can lead to increased elongation [19, 38]. As shown in Fig. 7, both the strength and ductility were improved with increasing the GNPs content from 0 vol% to 0.5 vol% (Samples S1–S3). The improvement in elongation is attributed to the hindering effect of GNPs bridging, pulling out and flattening on crack propagation.

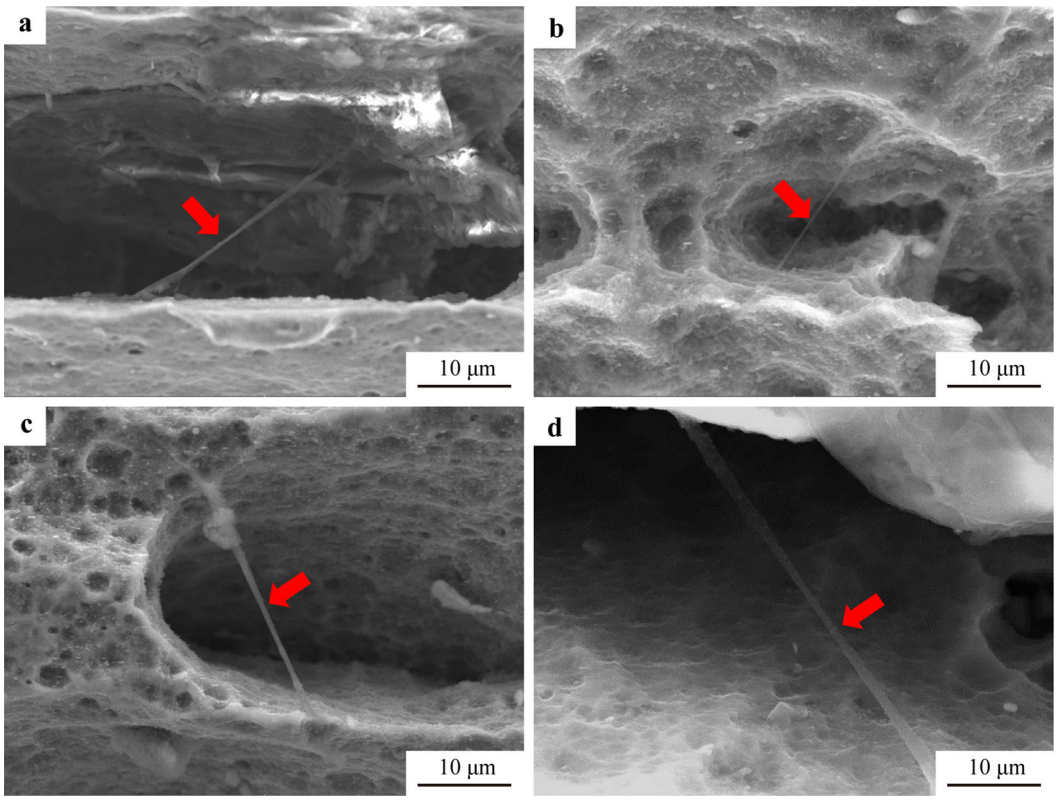

Fig. 9 SEM images showing GNPs bridging in composite Samples **a** S2, **b** S3, **c** S4 and **d** S5

5 Conclusion

GNPs/Al nanocomposites were fabricated from GNPs and pure Al sheets by using an accumulative roll-compositing process that is featured by ultrahigh rolling cycles. Microstructures, mechanical properties and electrical conductivity of the samples were investigated.

We showed that the ARC process enabled the fabrication of bulk GNPs/Al nanocomposites with a uniform dispersion of GNPs in the ultrafine-grained Al matrix. A small amount of GNPs addition (0.2 vol% and 0.5 vol%) can lead to both higher strength and higher ductility than the ARCed pure Al. The nanocomposite with 2.0 vol% GNPs exhibited a strength of 387 MPa, about 4.5 and 3.0 times those of annealed Al and ARCed Al. The present GNPs/Al nanocomposites exhibited an excellent balance between mechanical properties and electrical property. The strength ranged from 250 to 387 MPa, elongation from 15% to 20% and electrical conductivity from 28 to 31 $MS{\cdot}m^{-1}$. The excellent performance of the present nanocomposites is associated with the unique ARC process that enabled the uniform dispersion of GNPs in the ultrafine-grained Al matrix.

Acknowledgments This work was financially supported by the National Natural Science Foundation of China (No. 51371128) and the Fundamental Research Funds for the Central Universities of China (No. 2042017KF0190).

References

[1] Ma ZY, Tjong SC. In situ ceramic particle-reinforced aluminum matrix composites fabricated by reaction pressing in the TiO_2 (Ti)-Al-B (B_2O_3) systems. Metall Mater Trans A. 1997;28(9):1931.
[2] Liu YQ, Fan JZ, Hao XX, Wei SH, Nie JH, Ma ZL, Liu MK, Wang YB. Advanced hermetic electronic packaging based on lightweight silicon/aluminum composite produced by powder metallurgy technique. Rare Met. 2020;39(11):1307.
[3] Feng SY, Li QL, Liu W, Shu GG, Wang X. Microstructure and mechanical properties of Al-B_4C composite at elevated temperature strengthened with in situ Al_2O_3 network. Rare Met. 2020;39(6):671.
[4] Gao HD, Wang ZH, Shao J. Manufacture and characteristics of Al_2O_3 composite coating on steel substrate by SHS process. Rare Met. 2019;38(7):704.
[5] Bi GL, Han YX, Jiang J, Jiang CH, Li YD, Ma Y. Microstructural evolution and age-hardening behavior of quasicrystal-reinforced Mg-Dy-Zn alloy. Rare Met. 2019;38(8):739.
[6] Baig Z, Mamat O, Mustapha M. Recent progress on the dispersion and the strengthening effect of carbon nanotubes and graphene-reinforced metal nanocomposites: a review. Crit Rev Solid State Mater Sci. 2018;43(1):1.
[7] Tjong SC. Recent progress in the development and properties of novel metal matrix nanocomposites reinforced with carbon nanotubes and graphene nanosheets. Mater Sci Eng R Reports. 2013;74(10):281.

[8] Kuzumaki T, Miyazawa K, Ichinose H, Ito K. Processing of carbon nanotube reinforced aluminum composite. J Mater Res. 1998;13(09):2445.
[9] Izadi H, Gerlich AP. Distribution and stability of carbon nanotubes during multi-pass friction stir processing of carbon nanotube/aluminum composites. Carbon. 2012;50(12):4744.
[10] Li PB, Tan WT, Gao MM, Liu KG. Semisolid microstructural evolution of (CNTs + Si_p)/AZ91D powder compacts prepared from powders by cold pressing and remelting. Rare Met. 2020; 39(6):733.
[11] Kim KT, Eckert J, Menzel SB, Gemming T, Hong SH. Grain refinement assisted strengthening of carbon nanotube reinforced copper matrix nanocomposites. Appl Phys Lett. 2008;92(12): 121901.
[12] Honma T, Nagai K, Katou A, Arai K, Suganuma M, Kamado S. Synthesis of high-strength magnesium alloy composites reinforced with Si-coated carbon nanofibres. Scr Mater. 2009;60(6): 451.
[13] Shimizu Y, Miki S, Soga T, Itoh I, Todoroki H, Hosono T, Sakaki K, Hayashi T, Kim KA, Endo M, Morimoto S, Koide A. Multi-walled carbon nanotube-reinforced magnesium alloy composites. Scr Mater. 2008;58(4):267.
[14] Kwon H, Estili M, Takagi K, Miyazaki T, Kawasaki A. Combination of hot extrusion and spark plasma sintering for producing carbon nanotube reinforced aluminum matrix composites. Carbon. 2009;47(3):570.
[15] Morovvati MR, Mollaei-Dariani B. The formability investigation of CNT-reinforced aluminum nano-composite sheets manufactured by accumulative roll bonding. Int J Adv Manuf Technol. 2018;95(9–12):3523.
[16] Tokutomi J, Uemura T, Sugiyama S, Shiomi J, Yanagimoto J. Hot extrusion to manufacture the metal matrix composite of carbon nanotube and aluminum with excellent electrical conductivities and mechanical properties. CIRP Ann. 2015;64(1): 257.
[17] Bartolucci SF, Paras J, Rafiee MA, Rafiee J, Lee S, Kapoor D, Koratkar N. Graphene–aluminum nanocomposites. Mater Sci Eng, A. 2011;528(27):7933.
[18] Wang J, Li Z, Fan G, Pan H, Chen Z, Zhang D. Reinforcement with graphene nanosheets in aluminum matrix composites. Scr Mater. 2012;66(8):594.
[19] Li JL, Xiong YC, Wang XD, Yan SJ, Yang C, He WW, Chen JZ, Wang SQ, Zhang XY, Dai SL. Microstructure and tensile properties of bulk nanostructured aluminum/graphene composites prepared via cryomilling. Mater Sci Eng, A. 2015;626:400.
[20] Gao X, Yue H, Guo E, Zhang H, Lin X, Yao L, Wang B. Preparation and tensile properties of homogeneously dispersed graphene reinforced aluminum matrix composites. Mater Des. 2016;94:54.
[21] Shin SE, Choi HJ, Shin JH, Bae DH. Strengthening behavior of few-layered graphene/aluminum composites. Carbon. 2015;82: 143.
[22] Li M, Gao H, Liang J, Gu S, You W, Shu D, Wang J, Sun B. Microstructure evolution and properties of graphene nanoplatelets reinforced aluminum matrix composites. Mater Charact. 2018;140:172.
[23] Singhal SK, Pasricha R, Teotia S, Kumar G, Mathur RB. Fabrication and characterization of Al-matrix composites reinforced with amino-functionalized carbon nanotubes. Compos Sci Technol. 2011;72(1):103.
[24] Liu ZY, Xu SJ, Xiao BL, Xue P, Wang WG, Ma ZY. Effect of ball-milling time on mechanical properties of carbon nanotubes reinforced aluminum matrix composites. Compos Part A Appl Sci Manuf. 2012;43(12):2161.
[25] Li CL, Mei QS, Li JY, Chen F, Ma Y, Mei XM. Hall-Petch relations and strengthening of Al–ZnO composites in view of grain size relative to interparticle spacing. Scr Mater. 2018;153: 27.
[26] Zhang GP, Mei QS, Chen F, Ma Y, Mei XM, Li JY, Ruan XF, Wan L. Production of a high strength Al/($TiAl_3$ + Al_2O_3) composite from an Al-TiO_2 system by accumulative roll-bonding and spark plasma sintering. Mater Sci Eng, A. 2019;752:192.
[27] Bisht A, Srivastava M, Kumar RM, Lahiri I, Lahiri D. Strengthening mechanism in graphene nanoplatelets reinforced aluminum composite fabricated through spark plasma sintering. Mater Sci Eng, A. 2017;695:20.
[28] Zhao L, Lu H, Gao Z. Microstructure and mechanical properties of Al/graphene composite produced by high-pressure torsion. Adv Eng Mater. 2015;17(7):976.
[29] Rashad M, Pan F, Tang A, Asif M. Effect of graphene nanoplatelets addition on mechanical properties of pure aluminum using a semi-powder method. Prog Nat Sci Mater Int. 2014; 24(2):101.
[30] Liu SX. Practical Metal Materials Handbook. Beijing: China Machine Press; 2017. 701.
[31] Shen NF. New Handbook of Metallic Materials. Beijing: Science Press; 2003. 275.
[32] Zhang JY, Gao YH, Yang C, Zhang P, Kuang J, Liu G, Sun J. Microalloying Al alloys with Sc: a review. Rare Met. 2020; 39(6):636.
[33] Liu CY, Teng GB, Ma ZY, Wei LL, Zhou WB, Huang HF, Qi HQ. Mechanical properties and thermal stability of 7055 Al alloy by minor Sc addition. Rare Met. 2020;39(6):725.
[34] Nie JF, Muddle BC. Microstructural design of high-strength aluminum alloys. J Phase Equilibria. 1998;19(6):543.
[35] Yun C, Feng Y, Qiu T, Yang J, Li X, Yu L. Mechanical, electrical, and thermal properties of graphene nanosheet/aluminum nitride composites. Ceram Int. 2015;41(7):8643.
[36] Walker LS, Marotto VR, Rafiee MA, Koratkar N, Corral EL. Toughening in graphene ceramic composites. ACS Nano. 2011; 5(4):3182.
[37] Lee B, Koo MY, Jin SH, Kim KT, Hong SH. Simultaneous strengthening and toughening of reduced graphene oxide/alumina composites fabricated by molecular-level mixing process. Carbon. 2014;78:212.
[38] Yan SY, Dai SL, Zhang XY, Yang C, Hong QH, Chen JZ, Lin ZM. Investigating aluminum alloy reinforced by graphene nanoflakes. Mater Sci Eng, A. 2014;612:440.